LETTERS

PLETHORA proteins as dose-dependent master regulators of *Arabidopsis* root development

Carla Galinha[1]*†, Hugo Hofhuis[1]*, Marijn Luijten[1], Viola Willemsen[1], Ikram Blilou[1], Renze Heidstra[1] & Ben Scheres[1]

Factors with a graded distribution can program fields of cells in a dose-dependent manner[1,2], but no evidence has hitherto surfaced for such mechanisms in plants. In the *Arabidopsis thaliana* root, two *PLETHORA* (*PLT*) genes encoding AP2-domain transcription factors have been shown to maintain the activity of stem cells[3]. Here we show that a clade of four *PLT* homologues is necessary for root formation. Promoter activity and protein fusions of PLT homologues display gradient distributions with maxima in the stem cell area. PLT activities are largely additive and dosage dependent. High levels of PLT activity promote stem cell identity and maintenance; lower levels promote mitotic activity of stem cell daughters; and further reduction in levels is required for cell differentiation. Our findings indicate that PLT protein dosage is translated into distinct cellular responses.

During animal development, instructive molecules acquire a graded distribution and induce distinct cellular responses in a concentration-dependent manner. Whether similar mechanisms occur in plants has been controversial; dosage-sensitive action of plant hormones has been inferred only after external application[4]. Plant stem cell regions, which supply cells for the growing root and shoot systems[5], are potential sites of action for instructive gradients. Stem cells are maintained in local micro-environments, which are similar to animal stem cell niches[6]. Stem cell daughters undergo additional divisions in transit-amplifying cell compartments called meristems; when cells leave the meristem they rapidly expand and differentiate. The *PLETHORA1* (*PLT1*, At3g20840) and *PLT2* (At1g51190) genes encode AP2-domain transcription factor family members essential for defining the root stem cell niche[3]. *plt1*;*plt2* mutants display stem cell loss, loss of transit-amplifying cells and reduced cell expansion. PLT1 and PLT2 expression strongly correlates with a transcriptional response maximum to the plant hormone auxin in the root tip[3,7] and this maximum has been shown to have profound organizing activity[8]—a property often associated with sources of instructive gradients. Here, we reveal that the *PLT* gene family controls distinct aspects of root development in a dose-dependent manner through PLT expression gradients that culminate in the stem cell niche.

The proteins encoded by At5g10510/*AINTEGUMENTA-LIKE6* (*AIL6*)/*PLT3* and At5g17430/*BABY BOOM*(*BBM*) group with PLT1 and PLT2 in the AP2/ERF transcription factor family (Supplementary Fig. 1)[9], and these candidate redundant factors are predicted to be expressed in the root[10].

From the heart-stage of embryogenesis onward, *PLT3* is expressed in provascular cells, the quiescent centre and columella progenitor cells (Fig. 1a). Post-embryonically, *PLT3* messenger RNA accumulates in the root stem cell niche with the strongest signal in the columella stem cell layer (Fig. 1b), in contrast to the predominant quiescent-centre-localization of *PLT1* and *PLT2* transcript[3]. At the heart-stage of embryo development, *BBM* is expressed in provascular cells and in the lens-shaped quiescent centre progenitor cell (Fig. 1c). Post-embryonically, *BBM* transcript accumulates in the quiescent centre and columella stem cells—in a similar manner to the *PLT* mRNAs—and in provascular cells of the proximal meristem (Fig. 1d).

The *plt3-1* mutant allele carries a T-DNA insertion interrupting the first AP2 domain (Supplementary Fig. 2). No transcript was detected by PCR with reverse transcription (RT–PCR) or by *in situ* hybridization on *plt3-1* seedlings (data not shown), suggesting that *plt3-1* is a null allele. Homozygous *plt3* single mutants have slightly shorter roots and meristems compared to wild type, but $plt1^{-/-}plt2^{-/-}plt3^{-/-}$ triple homozygotes are rootless (Fig. 1e, upper inset). Progeny from $plt1^{-/-}plt2^{-/-}plt3^{+/-}$, $plt1^{-/-}plt2^{+/-}plt3^{-/-}$ and $plt1^{+/-}plt2^{-/-}plt3^{-/-}$ plants segregate ~25% rootless triple mutants (Supplementary Table 2), demonstrating linkage between the rootless phenotype and the three *PLT* genes. The embryonic root pole of triple homozygous seedlings is fully differentiated at 3 days post germination (d.p.g.) and adventitious root primordia arrest at 6 d.p.g. (Supplementary Fig. 3). Mature $plt1^{-/-}plt2^{-/-}$ embryos have only subtle defects in the cellular organization of the distal-most region[3] (Supplementary Fig. 4), but $plt1^{+/-}plt2^{-/-}plt3^{-/-}$ parents yield ~25% embryos with aberrant root poles that lack a lateral root cap cell layer (Supplementary Fig. 4).

We previously showed that $plt1^{-/-}plt2^{-/-}$ mutants have strongly reduced transcription of the *PIN4* gene, which encodes an auxin efflux facilitator[11]. In triple mutant embryos from $plt1^{+/-}plt2^{-/-}plt3^{-/-}$ parents, *PIN1* and *PIN3* mRNAs are strongly reduced (Fig. 1g–j and Supplementary Table 1). Post-embryonic *PIN2* mRNA is strongly reduced in triple mutant roots before differentiation (Fig. 1k, l). Therefore, PLT1, PLT2 and PLT3 redundantly control expression of multiple *PIN* genes in the embryonic and post-embryonic root.

bbm-1 and *bbm-2* mutant alleles carry T-DNA insertions before and in the beginning of the first AP2 domain, respectively (Supplementary Fig. 2). Truncated transcripts are detected by RT–PCR and may be translated, but genetic interactions (described below) suggest that the insertions cause loss-of-function effects. $plt3^{-/-}bbm^{-/-}$ double mutants have a shorter root and root meristem than either single mutant (Fig. 1f, and Supplementary Fig. 3).

Intriguingly, the progeny of plants segregating different *plt* and *bbm* allele combinations lack root and hypocotyl (Fig. 1e, lower inset) at significant frequencies (Supplementary Table 2), reaching ~10% of the progeny of selfed $plt1^{-/-}plt2^{+/-}plt3^{-/-}bbm\text{-}2^{-/-}$. These defects initiate in the early basal embryo (Supplementary Fig. 5) and resemble those in mutants of the auxin response factor *MONOPTEROS*[12] and the auxin perception machinery[13,14]. *PLT* genes do not seem to strongly perturb early global auxin-dependent patterning processes, as suggested by essentially normal cotyledon vasculature in the triple mutant (Supplementary Fig. 4). Segregation

[1]Department of Biology, Faculty of Science, Utrecht University, Padualaan 8, 3584 CH Utrecht, The Netherlands. †Present address: Department of Plant Sciences, University of Oxford, South Parks Road, Oxford OX1 3RB, UK.
*These authors contributed equally to this work.

of *plt2* in a homozygous *bbm* background and vice versa yields ~25% early arrested embryos, and homozygous double mutants could not be recovered, indicating a redundant function in early embryogenesis (data not shown).

Ectopic root structures are initiated by constitutive embryonic expression of *PLT* genes[3] and after induction of *BBM* expression[15]. To test whether PLT induction induces a developmental switch to root development, we expressed a PLT2–GR fusion protein that complements $plt1^{-/-}plt2^{-/-}$ after dexamethasone (dex) induction, when driven by its own promoter (Supplementary Fig. 6). When *35S-PLT2–GR* is activated by application of dex, roots are produced from the shoot apex (Fig. 1m, n). Our gain- and loss-of-function experiments indicate that *PLT* genes are master switches for root development.

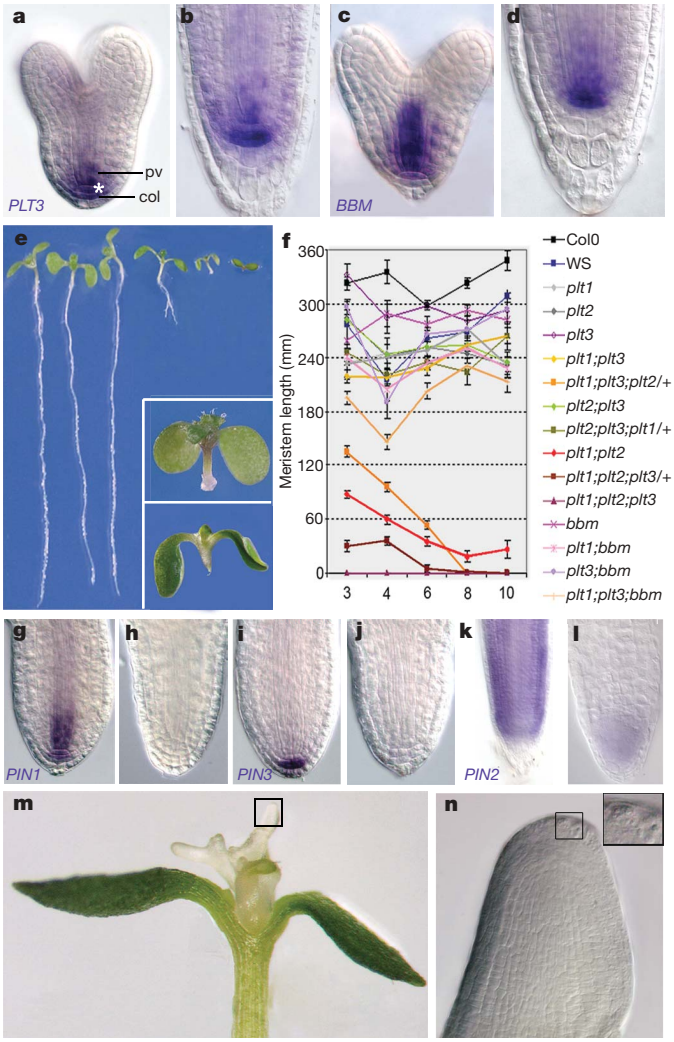

Figure 1 | Four *PLT* genes promote root formation. **a–d**, *In situ* hybridization with *PLT3*- (**a**, **b**) and *BBM*- (**c**, **d**) specific probes in wild-type embryos at heart-stage (**a**, **c**), and in roots of 3 d.p.g. wild-type plants (**b**, **d**). Asterisk, quiescent centre; pv, provasculature; col, columella. **e**, Seedlings 10 d.p.g., from left to right: wild type, $plt3^{-/-}$, $bbm\text{-}1^{-/-}$, $plt1^{-/-}plt2^{-/-}$, $plt1^{-/-}plt2^{-/-}plt3^{-/-}$ and a $plt1^{-/-}plt2^{+/-}plt3^{-/-}bbm\text{-}1^{-/-}$ segregant. Insets show magnification of $plt1^{-/-}plt2^{-/-}plt3^{-/-}$ mutant (upper) and $plt1^{-/-}plt2^{+/-}bbm\text{-}1^{-/-}$ segregant (lower). **f**, Meristem size in wild type (Col0 and WS) and *plt* mutants at the indicated d.p.g. For each data point, $n = 10$ to 50; error bars, s.e.m. **g–l**, *In situ* hybridization using PIN probes on wild-type (**g**, **i**) and $plt1^{-/-}plt2^{-/-}plt3^{-/-}$ (**h**, **j**) torpedo-stage embryos and wild-type (**k**) and $plt1^{-/-}plt2^{-/-}plt3^{-/-}$ mutant (**l**) 2 d.p.g. seedlings. **m**, Shoot of 9 d.p.g. *35S-PLT2–GR* plant 6 days after dexamethasone application. **n**, Magnification reveals cellular organization of ectopic root including columella starch granules.

$plt1^{-/-}plt2^{+/-}plt3^{-/-}$ mutants have intermediate root and meristem size between $plt1^{-/-}plt3^{-/-}$ and $plt1^{-/-}plt2^{-/-}plt3^{-/-}$ (Fig. 1e, f, and Supplementary Fig. 3) and 50% of $plt1^{-/-}plt2^{+/-}plt3^{-/-}bbm^{-/-}$ seedlings have shorter roots than $plt1^{-/-}plt3^{-/-}bbm^{-/-}$, whereas 50% have no primary root (Supplementary Table 2). *plt3* alleles are also semi-dominant, because growth and meristem maintenance defects in $plt1^{-/-}plt2^{-/-}plt3^{+/-}$ seedlings are intermediate between $plt1^{-/-}plt2^{-/-}$ and $plt1^{-/-}plt2^{-/-}plt3^{-/-}$ (Fig. 1f, and Supplementary Fig. 3). The semi-dominance of *plt2* and *plt3* loss-of-function alleles indicates dose-dependent activity.

To test whether *PLT* genes equally contribute to PLT 'dosage', we transformed $plt1^{-/-}plt2^{-/-}$ double mutants with *PLT1*, *PLT2*, *PLT3* and *BBM* genes fused to the yellow fluorescent protein gene *YFP* and driven by the full *PLT2* promoter. In independent lines with similar overall YFP levels, *PLT1* and *PLT2* fully complemented and *PLT3* and *BBM* partially complemented root growth in the double mutant. All PLT proteins rescued columella stem cell activity (Supplementary Figs 6 and 7). Thus, total PLT levels and to some extent intrinsic differences in PLT protein activity contribute to root growth and stem cell maintenance.

Transgenic lines carrying complete promoters of the *PLT* genes fused to the cyan fluorescent protein gene *CFP* reveal highest promoter activity in the stem cell niche, consistent with mRNA levels, but they also show graded activity in the proximal meristem (Fig. 2a–d). Gradients can be observed in epidermal surface views, excluding quenching effects, and they are specific to *PLT* promoters (Fig. 2e). To analyse whether this promoter activity drives a PLT protein gradient, we combined the PLT–YFP fusions with their corresponding full promoters. *PLT1* and *PLT2* gene fusions complemented $plt1^{-/-}plt2^{-/-}$ mutants (Supplementary Figs 6 and 7, and data not shown).

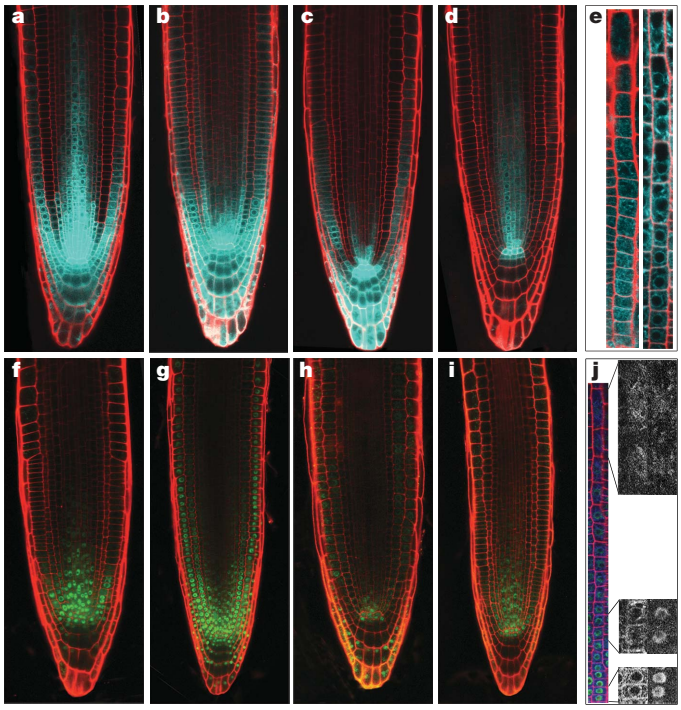

Figure 2 | *PLT* promoter activity and PLT protein fusions display gradients. **a–d**, CFP reporter driven by full-size promoters of *PLT1* (**a**) *PLT2* (**b**) *PLT3* (**c**) and *BBM* (**d**). **e**, Epidermal gradient of *PLT2* (left) but not *RCH2* (right) promoter. **f–i**, YFP reporter fused in-frame to genomic fragments of *PLT1* (**f**), *PLT2* (**g**), *PLT3* (**h**) and *BBM* (**i**). **j**, Co-localization in one plant of *PLT2* transcriptional (CFP, left magnification) and translational (YFP, right magnification) fusion viewed in different regions using separate channels.

All PLT protein fusions revealed conspicuous gradients that extend into the transit-amplifying cells and, for the PLT2 and PLT3 fusions, into the elongation zone (Fig. 2f–i). The promoter and protein gradients fully match when combined in one plant (Fig. 2j). We previously reported accumulation of *PLT* transcripts in the stem cell area[3], but, after extended staining, *PLT1 in situ* hybridizations also reveal a broader expression domain (Supplementary Fig. 8). We concluded that *PLT* promoter activity leads to protein gradients with maximum expression in the stem cell niche. PLT1 and PLT2 expression maxima broadly encompass the niche, whereas PLT3 and BBM are more restricted.

We asked whether differences in PLT expression domains affect the ability of PLT proteins to compensate for redundant partners. Indeed, *PLT1* and *PLT2* only partially complement a $plt1^{-/-}plt2^{-/-}$ mutant when driven by the *BBM* promoter (Supplementary Figs 6 and 7).

Our experiments suggested that the PLT protein concentration gradient instructs different outputs in different regions, even though each gene slightly differs in activity and expression profile. We therefore tested whether altering the level or shape of the PLT2 gradient affects the position of developmental boundaries. We expressed the PLT2–YFP fusion in $plt1^{-/-}plt2^{-/-}$ mutants under the *RCH2* promoter, which has low activity in the stem cell area but is active in meristematic and elongating cells at a level comparable to that of the *PLT2* promoter (Fig. 3d–g). *RCH2-PLT2–YFP* prolongs transit-amplifying cell divisions but fails to maintain stem cells at 7 d.p.g. (Fig. 3b, d). The transit-amplifying cell pool is lost at 12 d.p.g. (Fig. 3c). We concluded that intermediate PLT levels in the meristem promote transient cell cycling.

To validate that meristem size is controlled by a PLT gradient, we analysed $plt1^{-/-}plt2^{-/-}$ mutants complemented with the PLT2–YFP construct driven by a truncated 1.3-kb *PLT2* promoter fragment (*pPLT2s*). This truncated promoter drives significant expression in the stem cell area but the gradient declines more rapidly (Fig. 3e, f). Accordingly, stem cells are rescued but root and meristem sizes are ~50% smaller (Supplementary Fig. 7). The amount of YFP signal per mid-nuclear section in the stem cell zone, halfway the meristem, and in the first expanding cells, provides three clearly separated intensity ranges that match with zonation in the full- and truncated-promoter driven gradients (Fig. 3g), suggesting that the PLT2 gradient defines meristem zonation.

A dose-dependent gradient model predicts that PLT overexpression shifts the meristem boundary. Indeed, dex induction of *35S-PLT2–GR* plants promotes continuous growth of the transit-amplifying cell pool and meristem size increases (Fig. 4a–c). Ink toner marks marking the elongation zone boundaries at the time of induction reveal that PLT overexpression sustains cell division only in cells that are still cycling and inhibits cell expansion in the elongation zone. These data reinforce the idea that distinct PLT levels dictate cell proliferation and mitotic exit.

The auxin response marker *DR5-GUS*[8] and *PIN3* transcription do not change in *35S-PLT2–GR* plants just before the onset of meristem size expansion, but only at later stages, indicating that PLT-induced expansion of the division zone is not caused by rapid changes in *PIN* expression (Supplementary Fig. 9).

Notably, the stem cell area in PLT2–GR plants is not altered after induction (Fig. 4c). The *RETINOBLASTOMA* (*RBR*) pathway was recently identified as an independent stem cell input[16], so we reasoned that this pathway might still limit stem cell pool size in the presence of higher PLT levels. Therefore, we combined a root-specific RNA interference (RNAi)-mediated silencing construct (*RCH1-RBRi*)[16] with *35S-PLT2–GR*. After induction with dex in the double transgenic, root meristem size increases as in *35S-PLT2–GR*, but clusters of dividing cells in the root cap area expand beyond that seen in *RCH1-RBRi* alone (Fig. 4d, e). Moreover, periclinal divisions normally associated with stem cells occur throughout the proximal area (Fig. 4f). These data suggested that the high expression region of the PLT gradient can be instructive for stem cell fate. Dramatic support for this notion is provided by duplications of the distal stem cell area in ~10% of *RCH1-RBRi;35S-PLT2–GR* root meristem zones (Fig. 4g–i). We concluded that high PLT levels define the stem cell domain, confirming PLT dosage-dependent stem cell specification.

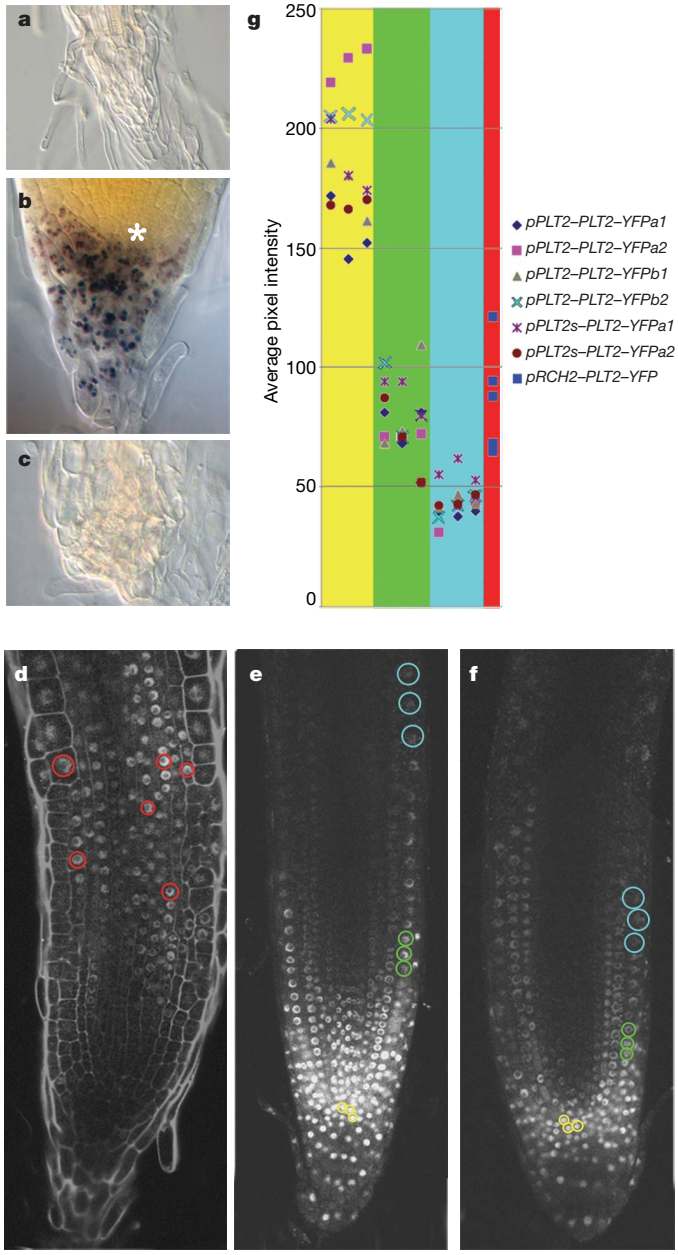

Figure 3 | PLT expression regulates stem cell maintenance and meristem boundary. a–d, Meristem prolongation but not stem cell rescue in *RCH2-PLT2–YFP* plants. Nomarski optics image of root tip of 7 d.p.g. *plt1;plt2* (**a**), and of *plt1;plt2 RCH2-PLT2–YFP* at 7 d.p.g. (**b**) and 12 d.p.g. (**c**). Starch granule staining (brown) shows no rescue of columella stem cells below the quiescent centre. Confocal view of 7 d.p.g. *plt1;plt2 RCH2-PLT2–YFP* root (**d**) shows that the meristem is rescued and reveals no expression of PLT2–YFP in the stem cell area. Asterisk in **b**, quiescent centre. **e, f**, Promoter truncation shifts the meristem boundary. CLSM views at identical pinhole and laser settings for *RCH2-PLT2–YFP* (**d**), *pPLT2-PLT2–YFP* (**e**) and *pPLT2s-PLT2–YFP* (**f**). **g**, Quantification of fluorescence per nucleus in *pRCH2-PLT2–YFP* transient meristem (red circles in **d**, and red graph areas), and in stem cells (yellow in **e, f** and graph area), mid-meristem (green in **e, f** and graph area) and first elongating cells (blue in **e, f** and graph area) of *pPLT2-PLT2–YFP* and pPLT2s-PLT2–YFP (a and b indicate independent transformants, 1 and 2 indicate different roots).

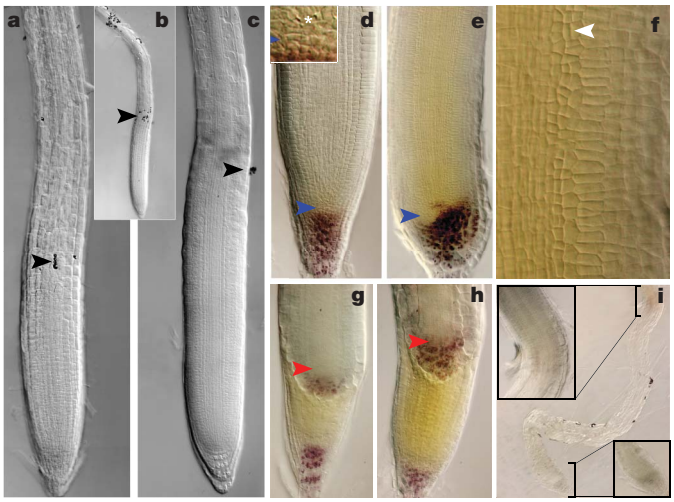

Figure 4 | Inducible expansion of meristem and stem cell area with PLT2–GR fusions. **a–c**, *35S-PLT2–GR* 7 d.p.g. without dex (**a**) and 1 d after 5 μM dex application (**b**, **c**). Overview shows positioning of ink toner particles that mark the meristem boundary (black arrowhead) and upper elongation zone boundary at the onset of induction (**b**); the elongation zone boundary is defined as the position where cortical cells rapidly expand. Induced PLT2–GR roots reveal cell division below the meristem boundary and incomplete cell elongation (**c**). **d–f**, *35S-PLT2–GR*;*pRCH1-RBR* RNAi plants: 10 d.p.g. without dex revealing the two *RBRi*-induced stem cell layers below the quiescent centre (blue arrowhead, inset), asterisk indicates the quiescent centre (**d**); with 3 d of dex application, revealing excessive root cap stem cells (blue arrowhead) and periclinal divisions in the proximal meristem (**e**); magnification with ectopic periclinal divisions (**f**, white arrowhead). **g–i**, Duplication of the stem cell area (red arrowheads) and distal cell types (brown starch granules) in ~10% of 8 d.p.g. *35S-PLT2–GR*, *pRCH1-RBRi* plants after dex application. Early (**g**), mid- (**h**) and late (**i**) stages of ectopic stem cell centre; note the prolonged activity of both stem cell centres (**i**, inset).

This effect is normally limited by RBR. Low RBR levels in the *RCH1-RBRi* transgenic display limited expansion of the stem cell domain[16] because the PLT levels dictated by the gradient are limiting.

Our data indicate that PLT protein gradients define three outputs in the growing root primordium: stem cell programming, mitotic activity and exit to differentiation. Analysis of PLT target genes will be required to assess how much of the response to graded activity is due to additive concentration effects on the same targets and to differences in target specificity.

Although the molecular link between auxin action and *PLT* gene activation may not be direct[3], auxin distribution and response systems are essential for correct *PLT* gene transcription. This raises the possibility that PLT proteins promote stem cells and transit-amplifying cells as a graded read-out of auxin distribution. In an accompanying paper, we provide evidence that PIN-mediated polar auxin transport establishes a dynamic gradient spanning the root meristem[17]. Hence it is tempting to speculate that an auxin gradient underlies the observed PLT gradients. Classical morphogen systems were conceptualized as independent from the response system. However, several gradients in animal development involve complicated dynamics (for example, ref. 18) and the static concept of positional information is being challenged[19]. We show that PIN polar auxin transport facilitator expression that is essential for correct auxin distribution is regulated by PLT activity, which is a clear example of entanglement between positional information and its response system.

METHODS SUMMARY

Plant work. *plt1-4* and *plt2-2* alleles were described in ref. 3, *plt3-1*, and *bbm-1* and *bbm-2* are salk T-DNA insertion lines 127417, 097021 and 067917, respectively, provided by the Signal Insertion Mutant Library (http://signal.salk.edu/). The T-DNA insertion in *PLT3* was confirmed by genotyping. The *plt1*;*plt2*;*plt3* triple mutant was generated by crossing *plt3-1* to *plt1-4*;*plt2-2*. *bbm-1* and *bbm-2* were crossed to *plt1-4*;*plt2-2* and *plt3-1* and allelic combinations were selected from F_2 populations. The T-DNA insertion site on *bbm-1* and *bbm-2* lines was verified by genotyping. Primers for genotyping are indicated in Supplementary Table 3. Promoter and genomic sequences were amplified from Col-0 genomic DNA using the primer combinations listed in Supplementary Table 3.. Promoter fragments were fused to the endoplasmic reticulum targeted CFP coding sequence in a pGreenII vector[20]. For translational fusions, *PLT* genomic sequences were fused at the 3′ end to either the *YFP* coding sequence or the carboxy-terminal-encoding region of the rat glucocorticoid (GR) receptor[21] and placed under the control of particular promoters (amplified regions are described in Supplementary Table 3). Promoter swaps were performed by fusing 5.8 kb of *PLT2* and 4.2 kb of *BBM* promoter fragments to the *YFP*-fused *PLT* genomic sequences. Transgenic plants were generated by transforming Col-0 wild-type or *plt1-4*;*plt2-2* plants, as described[22].

Phenotype analysis and microscopy. Light microscopy[23], confocal microscopy and aniline blue staining[24] of mature embryos was performed as described. Root length was measured, as before[3]. Meristem cell length was measured using ImageJ (v.1.36) and mature cortical cell length as well as fluorescence levels were determined using Zeiss LSM Pascal (3.2SP2) software.

***In situ* hybridization.** Whole-mount RNA *in situ* hybridization was performed as described[11]. The *PLT3* and *BBM* riboprobes, specific for non-conserved sequences downstream of the AP2 repeats, were prepared from templates amplified from complementary DNA (for primers, see Supplementary Table 3). The *PLT1* probe is as in ref. 3; the *PIN1*, *PIN2* and *PIN3* probes are as in ref. 25.

Received 5 July; accepted 30 August 2007.

1. Tabata, T. & Takei, Y. Morphogens, their identification and regulation. *Development* **131,** 703–712 (2004).
2. Gurdon, J. B. & Bourillot, P. Y. Morphogen gradient interpretation. *Nature* **413,** 797–803 (2001).
3. Aida, M. *et al.* The *PLETHORA* genes mediate patterning of the *Arabidopsis* root stem cell niche. *Cell* **119,** 109–120 (2004).
4. Skoog, F. & Miller, C. O. Chemical regulation of growth and organ formation in plant tissues cultured *in vitro*. *Symp. Soc. Exp. Biol.* **54,** 118–130 (1957).
5. Weigel, D. & Jurgens, G. Stem cells that make stems. *Nature* **415,** 751–754 (2002).
6. Spradling, A., Drummond-Barbosa, D. & Kai, T. Stem cells find their niche. *Nature* **414,** 98–104 (2001).
7. Xu, J. *et al.* A molecular framework for plant regeneration. *Science* **311,** 385–388 (2006).
8. Sabatini, S. *et al.* An auxin-dependent distal organizer of pattern and polarity in the *Arabidopsis* root. *Cell* **99,** 463–472 (1999).
9. Nole-Wilson, S., Tranby, T. L. & Krizek, B. A. AINTEGUMENTA-like (*AIL*) genes are expressed in young tissues and may specify meristematic or division-competent states. *Plant Mol. Biol.* **57,** 613–628 (2005).
10. Birnbaum, K. *et al.* A gene expression map of the *Arabidopsis* root. *Science* **302,** 1956–1960 (2003).
11. Blilou, I. *et al.* The PIN auxin efflux facilitator network controls growth and patterning in *Arabidopsis* roots. *Nature* **433,** 39–44 (2005).
12. Hardtke, C. S. & Berleth, T. The *Arabidopsis* gene *MONOPTEROS* encodes a transcription factor mediating embryo axis formation and vascular development. *EMBO J.* **17,** 1405–1411 (1998).
13. Hellmann, H. *et al.* *Arabidopsis AXR6* encodes CUL1 implicating SCF E3 ligases in auxin regulation of embryogenesis. *EMBO J.* **22,** 3314–3325 (2003).
14. Dharmasiri, N. *et al.* Plant development is regulated by a family of auxin receptor F box proteins. *Dev. Cell* **9,** 109–119 (2005).
15. Srinivasan, C. *et al.* Heterologous expression of the BABY BOOM AP2/ERF transcription factor enhances the regeneration capacity of tobacco (*Nicotiana tabacum* L.). *Planta* **225,** 341–351 (2007).
16. Wildwater, M. *et al.* The *RETINOBLASTOMA-RELATED* gene regulates stem cell maintenance in *Arabidopsis* roots. *Cell* **123,** 1337–1349 (2005).
17. Grieneisen, V. A., Xu, J., Marée, A. F. M., Hogeweg, P. & Scheres, B. Auxin transport is sufficient to generate a maximum and gradient guiding root growth. *Nature* doi:10.1038/nature06215 (this issue).
18. O'Connor, M. B., Umulis, D., Othmer, H. G. & Blair, S. S. Shaping BMP morphogen gradients in the *Drosophila* embryo and pupal wing. *Development* **133,** 183–193 (2006).
19. Jaeger, J. & Reinitz, J. On the dynamic nature of positional information. *Bioessays* **28,** 1102–1111 (2006).
20. Hellens, R. P., Edwards, E. A., Leyland, N. R., Bean, S. & Mullineaux, P. M. pGreen: a versatile and flexible binary Ti vector for *Agrobacterium*-mediated plant transformation. *Plant Mol. Biol.* **42,** 819–832 (2000).
21. Aoyama, T. & Chua, N. H. A glucocorticoid-mediated transcriptional induction system in transgenic plants. *Plant J.* **11,** 605–612 (1997).

22. Clough, S. J. & Bent, A. F. Floral dip: a simplified method for *Agrobacterium*-mediated transformation of *Arabidopsis* thaliana. *Plant J.* **16,** 735–743 (1998).
23. Willemsen, V., Wolkenfelt, H., deVries, G., Weisbeek, P. & Scheres, B. The *HOBBIT* gene is required for formation of the root meristem in the *Arabidopsis* embryo. *Development* **125,** 521–531 (1998).
24. Bougourd, S., Marrison, J. & Haseloff, J. Technical advance: an aniline blue staining procedure for confocal microscopy and 3D imaging of normal and perturbed cellular phenotypes in mature *Arabidopsis* embryos. *Plant J.* **24,** 543–550 (2000).
25. Friml, J. *et al.* AtPIN4 mediates sink-driven auxin gradients and root patterning in *Arabidopsis*. *Cell* **108,** 661–673 (2002).

Supplementary Information is linked to the online version of the paper at www.nature.com/nature.

Acknowledgements We thank the Netherlands Genomics Initiative (M.L.) and the Portuguese Foundation for Science and Technology (C.G.) for funding, A. Shimotohno and J. M. Perez-Perez for sharing data and Frits Kindt for photography.

Author Information Reprints and permissions information is available at www.nature.com/reprints. Correspondence and requests for materials should be addressed to B.S. (b.scheres@uu.nl).